Journal of Pain Research

Dovepress
Taylor & Francis Group

Open Access Full Text Article

ORIGINAL RESEARCH

Peripheral Sympathetic Sprouting Drives Neuropathic Pain via Spinal Microglial P2Y12 Activation in a Rat Spinal Nerve Ligation Model

Tingting Yu[1], Huan Huang[1], Zhipeng Li[2], Hai Yan[1]

[1]Department of Anesthesiology, Shanghai Jiao Tong University Affiliated Sixth People's Hospital, Shanghai, People's Republic of China; [2]Shanghai Key Laboratory of Sleep Disordered Breathing, Department of Otolaryngology-Head and Neck Surgery, Otolaryngology Institute of Shanghai Jiao Tong University, Shanghai Sixth People's Hospital Affiliated to Shanghai Jiao Tong University School of Medicine, Shanghai, People's Republic of China

Correspondence: Hai Yan, Email yanhai2000@126.com

Background: Sympathetically maintained pain (SMP) is heterogeneous, and sympathetic sprouting is not universal across neuropathic pain states. In the rat spinal nerve ligation (SNL) model, peripheral sympathetic-sensory coupling may amplify spinal neuroinflammation. We examined whether peripheral sympathetic drive and spinal microglial P2Y12 signaling operate as parallel pathways or as a coupled peripheral-to-central axis.

Methods: Male Sprague-Dawley rats were assigned to Sham, SNL, SNL + 6-OHDA, SNL + intrathecal ticagrelor, ticagrelor-only, or SNL + combined 6-OHDA/ticagrelor groups. Mechanical allodynia, microglial morphology, P2Y12/Iba-1 expression, p38 MAPK phosphorylation, and spinal cytokines were assessed by von Frey testing, immunofluorescence, Western blotting, and ELISA. A pharmacological occlusion paradigm tested pathway additivity.

Results: SNL produced marked ipsilateral mechanical allodynia. On postoperative day 7, 6-OHDA increased paw withdrawal threshold from 3.56 to 8.43 g (Hedges' g=2.56, 95% CI 1.03 to 4.10) and reduced SNL-induced spinal P2Y12, Iba-1, p-p38/t-p38, and TNF-α/IL-1β/IL-6 increases. Intrathecal ticagrelor similarly attenuated allodynia (4.64 to 7.84 g; Hedges' g=1.45, 95% CI 0.23 to 2.67). In the occlusion experiment, AUCs were higher in SNL + 6-OHDA (50.11±4.94 g.day), SNL + ticagrelor (55.83±10.79 g.day), and combined treatment (52.85 ±9.28 g.day) than in SNL (25.09±8.78 g.day), with no additional benefit of combination therapy.

Conclusion: These findings support a functional peripheral-to-central neuroimmune axis in which peripheral sympathetic activity amplifies spinal microglial P2Y12-p38 signaling in the SNL model. Purinergic interfaces may represent potential SMP targets, but clinical translation requires further validation.

Keywords: neuropathic pain, sympathetically maintained pain, microglia, P2Y12 receptor, sympathetic sprouting, spinal nerve ligation

Introduction

Neuropathic pain, resulting from lesions or disorders of the somatosensory system, is a severe and hard-to-treat condition. A clinically important subset of patients presents with sympathetically maintained pain (SMP), a heterogeneous phenomenon that is typically identified by pain relief after sympathetic blockade rather than by a single universal mechanism. In selected proximal nerve injury models, particularly spinal nerve ligation (SNL), aberrant postganglionic sympathetic fibers arising from sympathetic ganglia sprout into the dorsal root ganglion (DRG)[1] and form perisomatic networks around primary sensory neurons.[2–4] This sympathetic-sensory coupling can enhance primary afferent excitability, promote ectopic activity, and increase nociceptive input to the spinal cord.[3,5] However, because sympathetic sprouting is model-dependent and not universal across neuropathic pain states, its relationship to central neuroimmune activation requires careful experimental definition.

At the central level, neuropathic pain chronification involves central sensitization within the spinal dorsal horn. This process is not mediated by a single cell type but emerges from interactions among microglia, astrocytes, neurons, and, in some settings, peripheral immune cells.[6,7] Microglia are critical early responders to nerve injury, and the purinergic P2Y12 receptor

https://doi.org/10.2147/JPR.S608956
Received: 17 March 2026
Accepted: 9 June 2026
Published: 16 June 2026

is an important sensor of extracellular nucleotides released from hyperactive afferent terminals.[8] P2Y12 signaling primarily mediates microglial chemotaxis and early morphological responses, while downstream cytokine production is regulated by multiple convergent pathways, including but not limited to p38 MAPK-related signaling.[9] Thus, the P2Y12-p38 pathway is best viewed as a modulatory gateway within a broader neuroimmune network rather than as the sole direct driver of inflammatory cytokine synthesis.[10,11]

The peripheral sympathetic system and spinal microglia reside in anatomically distinct compartments. Peripheral sympathetic postganglionic fibers do not directly innervate the spinal cord parenchyma, and the blood-spinal cord barrier (BSCB) imposes additional compartmental constraints.[12,13] A key unresolved question is therefore whether peripheral sympathetic hyperactivity within the DRG can functionally amplify spinal microglial P2Y12 signaling, and whether these peripheral and central mechanisms behave as independent parallel pathways or as a coupled pharmacological sequence. This issue is clinically relevant because interventions directed only at the peripheral sympathetic system or only at central sensitization often provide incomplete or unsustained analgesia in refractory SMP.

In the present study, we used the rat L5 SNL model to test the hypothesis that peripheral sympathetic activity acts as a critical upstream amplifier of spinal microglial P2Y12-p38 signaling. We combined systemic peripheral chemical sympathectomy with intrathecal P2Y12 antagonism and used an in vivo pharmacological occlusion paradigm to assess additivity. We acknowledge that microglial activation can occur independently of sympathetic sprouting through direct nerve injury and neuron-glia signaling. Accordingly, our aim was not to claim a mandatory universal pathway, but to determine whether the sympathetic drive contributes to and functionally couples with spinal microglial P2Y12 signaling in this SMP-relevant preclinical model.

Materials and Methods

Study Design and Experimental Groups

This preclinical animal study used a rat L5 SNL model to examine whether peripheral sympathetic depletion and central P2Y12 antagonism affect overlapping or additive components of neuropathic pain. Depending on the specific experiment, rats were assigned to Sham, SNL, SNL + 6-OHDA, SNL + intrathecal ticagrelor, ticagrelor-only, or SNL + combined 6-OHDA/ticagrelor groups. The primary behavioral outcome was ipsilateral paw withdrawal threshold (PWT) to von Frey stimulation. Secondary outcomes included immunofluorescence-based microglial reactivity/morphology, P2Y12, Iba-1, p-p38/t-p38, and spinal TNF-α, IL-1β, and IL-6 levels.

Animals and Ethics Statement

Adult male Sprague-Dawley rats weighing 200–250 g at the beginning of the study were housed in a temperature-controlled room (22 ± 1°C) with a 12-hour light/dark cycle and ad libitum access to food and water. All animal experiments and surgical procedures were approved by the Animal Care and Use Committee of the Sixth People's Hospital Affiliated to Shanghai Jiao Tong University (SYXK [Shanghai, China] 2021–0028). Experiments were conducted in accordance with the National Institutes of Health guidelines for laboratory animal care and use and the ARRIVE guidelines. All efforts were made to minimize animal suffering and reduce animal use.

Randomization, Allocation Concealment, and Blinding

Animals were randomly assigned to experimental groups using a computer-generated random number sequence before surgery or pharmacological intervention. Allocation concealment was maintained by an independent researcher who prepared 6-OHDA, ticagrelor, or vehicle in identical coded syringes. Investigators performing surgery, intrathecal injections, behavioral testing, immunofluorescence quantification, Western blot densitometry, and ELISA measurements were blinded to group allocation until final data integration.

Sample Size Determination

Sample sizes were determined from comparable SNL literature and previous laboratory experience rather than a formal a priori power calculation. Behavioral experiments used n = 6–8 animals per group, whereas molecular and biochemical

assays used n = 4–6 samples per group, depending on assay feasibility and tissue availability. These values were selected to detect robust, biologically meaningful changes while observing the animal welfare principle of reduction. The absence of a formal power calculation is acknowledged as a limitation.

Spinal Nerve Ligation Model

The neuropathic pain model was established by L5 SNL. Rats were anesthetized with isoflurane (2–3% for induction and 1.5% for maintenance). After a midline lower back incision, the left L6 transverse process was removed to expose the L4 and L5 spinal nerves. The left L5 spinal nerve was tightly ligated with 6–0 silk suture. Sham-operated animals underwent identical nerve exposure without ligation.

Pharmacological Interventions

For systemic chemical sympathectomy, 6-hydroxydopamine (6-OHDA; Sigma-Aldrich, St. Louis, MO, USA) was dissolved in sterile 0.9% saline containing 0.1% ascorbic acid. Rats received a single intraperitoneal injection of 6-OHDA (100 mg/kg) 7 days before SNL; vehicle controls received saline/ascorbic acid. This preemptive schedule was used to minimize the possibility that post-injury BSCB disruption would confound interpretation. For central P2Y12 blockade, ticagrelor (Sigma-Aldrich) was dissolved in artificial cerebrospinal fluid containing DMSO (final concentration <5%) and administered intrathecally by lumbar puncture between L5 and L6 under brief isoflurane anesthesia. A reflexive tail flick indicated successful intrathecal entry. Ticagrelor was administered at 1 ug/10 uL followed by a 10 uL aCSF flush, once daily from postoperative day 1 to day 7. On behavioral testing days, ticagrelor was given 60 min before von Frey testing.

Behavioral Nociceptive Testing

Mechanical allodynia was assessed using calibrated von Frey filaments (Stoelting, USA) applied to the plantar surface of the hind paw. The 50% PWT was determined using the up-down method.[14] Behavioral testing was conducted by an investigator blinded to group allocation. Thermal hyperalgesia, cold allodynia, and spontaneous pain were not assessed.

Immunofluorescence Staining

At designated endpoints, rats were deeply anesthetized with an overdose of sodium pentobarbital (60 mg/kg, i.p). Unconsciousness was verified by absence of the righting reflex, and death was confirmed by cessation of breathing and absence of detectable heartbeat for at least 1 min before tissue collection. Animals were transcardially perfused with ice-cold PBS followed by 4% paraformaldehyde. Lumbar spinal cord segments (L4-L6) were collected, post-fixed, cryoprotected in 30% sucrose, and sectioned at 20 um. Sections were blocked with 5% normal goat serum containing 0.3% Triton X-100 and incubated overnight at 4°C with primary antibodies against CD11b (1:1000, Abcam), Iba-1 (1:500, Merck), P2Y12 (1:1000, Anaspec), and p-p38 (1:1000, CST). Fluorophore-conjugated Alexa Fluor 488/594 secondary antibodies were applied for 2 h at room temperature. Images were captured with an Olympus FV1000 confocal microscope and quantified using ImageJ. Because CD11b and Iba-1 do not specify microglial functional phenotype, they were interpreted as markers of microglial reactivity and morphology, with p-p38 and cytokine data used to infer inflammatory signaling. To verify peripheral sympathetic depletion, spleen sections (10 um) were stained for tyrosine hydroxylase (TH; 1:2000, Proteintech).

Western Blot Analysis

Lumbar spinal cord tissues (L4-L6) were homogenized in ice-cold RIPA buffer containing protease and phosphatase inhibitors. Equal amounts of protein (30 ug/lane) were separated by SDS-PAGE and transferred to PVDF membranes. Membranes were incubated overnight at 4°C with antibodies against P2Y12 (1:1000, Anaspec), Iba-1 (1:500, Merck), p-p38 (1:1000, CST), total p38 (1:1000, Abcam), and GAPDH (1:5000, Hangzhou HuaAn Biotechnology) as the loading control. Bands were detected by enhanced chemiluminescence and quantified using ImageJ. The relative phosphorylation level of p38 MAPK was expressed as the p-p38/t-p38 ratio.

Enzyme-Linked Immunosorbent Assay

Lumbar spinal cord tissues were homogenized in PBS containing protease inhibitors and centrifuged at 10,000 × g for 15 min at 4°C. Supernatants were collected, and total protein was quantified by BCA assay. TNF-α, IL-1β, and IL-6 were measured using commercially available rat ELISA kits (R&D Systems) according to the manufacturer instructions. Cytokine concentrations were normalized to total protein and expressed as pg/mg protein.

Statistical Analysis

Data are presented as mean ± SD unless otherwise stated. Statistical analyses were performed using GraphPad Prism 10. Normality and homogeneity of variance were assessed before applying parametric tests; when assumptions were satisfied, time-course von Frey data were analyzed using two-way repeated-measures ANOVA followed by Tukey post hoc testing. Molecular data and AUC values were analyzed using one-way ANOVA followed by the indicated post hoc test. A two-tailed $p < 0.05$ was considered statistically significant. To improve interpretability beyond p values, effect sizes were calculated for key between-group comparisons. Hedges' g is reported as the small-sample corrected standardized mean difference with 95% confidence intervals. Approximate thresholds of 0.2, 0.5, and 0.8 were interpreted as small, medium, and large effects, respectively. Comprehensive effect sizes are provided in Supplementary Table S1.

Results

Peripheral Chemical Sympathectomy Alleviates SNL-Induced Mechanical Allodynia

The experimental schedule for preemptive 6-OHDA administration, SNL surgery, behavioral testing, and tissue harvest is shown in Figure 1a. In the ipsilateral hind paw, SNL produced robust mechanical allodynia (Figure 1b). By postoperative day 7, ipsilateral PWT was reduced from 12.66 g in the sham group to 3.56 g in the SNL group (Hedges' g=−2.43, 95% CI −3.92 to −0.94). Preemptive systemic sympathectomy with 6-OHDA increased day 7 ipsilateral PWT from 3.56 g in SNL rats to 8.43 g (Hedges' g=2.56, 95% CI 1.03 to 4.10), indicating a large antiallodynic effect. In contrast, contralateral PWTs remained statistically unchanged among groups across the same time points (Figure 1c), supporting the laterality of the behavioral phenotype.

Peripheral Sympathetic Drive Modulates Spinal Microglial Reactivity and P2Y12-p38 Signaling

Representative immunofluorescence images showed that SNL induced a marked morphological shift of spinal dorsal horn microglia together with increased P2Y12 and CD11b signals, whereas systemic 6-OHDA reduced these changes (Figure 2a). Fluorescence quantification confirmed attenuation of SNL-induced P2Y12 and CD11b upregulation after 6-OHDA treatment (Figure 2b). Representative Western blots are shown in Figure 2c, and densitometric analyses demonstrated that 6-OHDA reduced SNL-induced P2Y12 expression (Figure 2d; Hedges' g=−2.59, 95% CI −4.13 to −1.04), Iba-1 expression (Figure 2e; Hedges' g=−3.70, 95% CI −5.63 to −1.77), and p-p38/t-p38 signaling (Figure 2f; Hedges' g=−1.96, 95% CI −3.32 to −0.61). ELISA analysis further showed parallel reductions in spinal TNF-α, IL-1β, and IL-6 after sympathetic depletion (Figure 2g). To directly verify the efficacy of peripheral sympathectomy, we examined splenic TH staining. Vehicle-treated control rats showed dense TH-positive sympathetic fibers (Figure S1a), whereas 6-OHDA-treated rats showed a marked loss of TH signal (Figure S1b). Quantification confirmed a reduction in relative TH fluorescence from 176.22±6.18 to 12.29±1.65 (Figure S1c; Hedges' g=−13.65, 95% CI −19.23 to −8.08), confirming successful peripheral sympathetic depletion.

Intrathecal P2Y12 Blockade Mitigates Neuropathic Pain and Dampens Microglial Inflammatory Signaling

The intrathecal ticagrelor schedule is summarized in Figure 3a. Intrathecal ticagrelor significantly attenuated SNL-induced ipsilateral mechanical allodynia (Figure 3b). On postoperative day 7, PWT increased from 4.64 g in SNL rats to 7.84 g after ticagrelor (Hedges' g=1.45, 95% CI 0.23 to 2.67). Contralateral PWTs did not differ significantly among groups, indicating that ticagrelor did not induce generalized changes in baseline mechanical sensitivity (Figure 3c). Representative Iba-1 and p-p38 immunofluorescence images showed that ticagrelor reduced SNL-associated microglial reactivity and p38

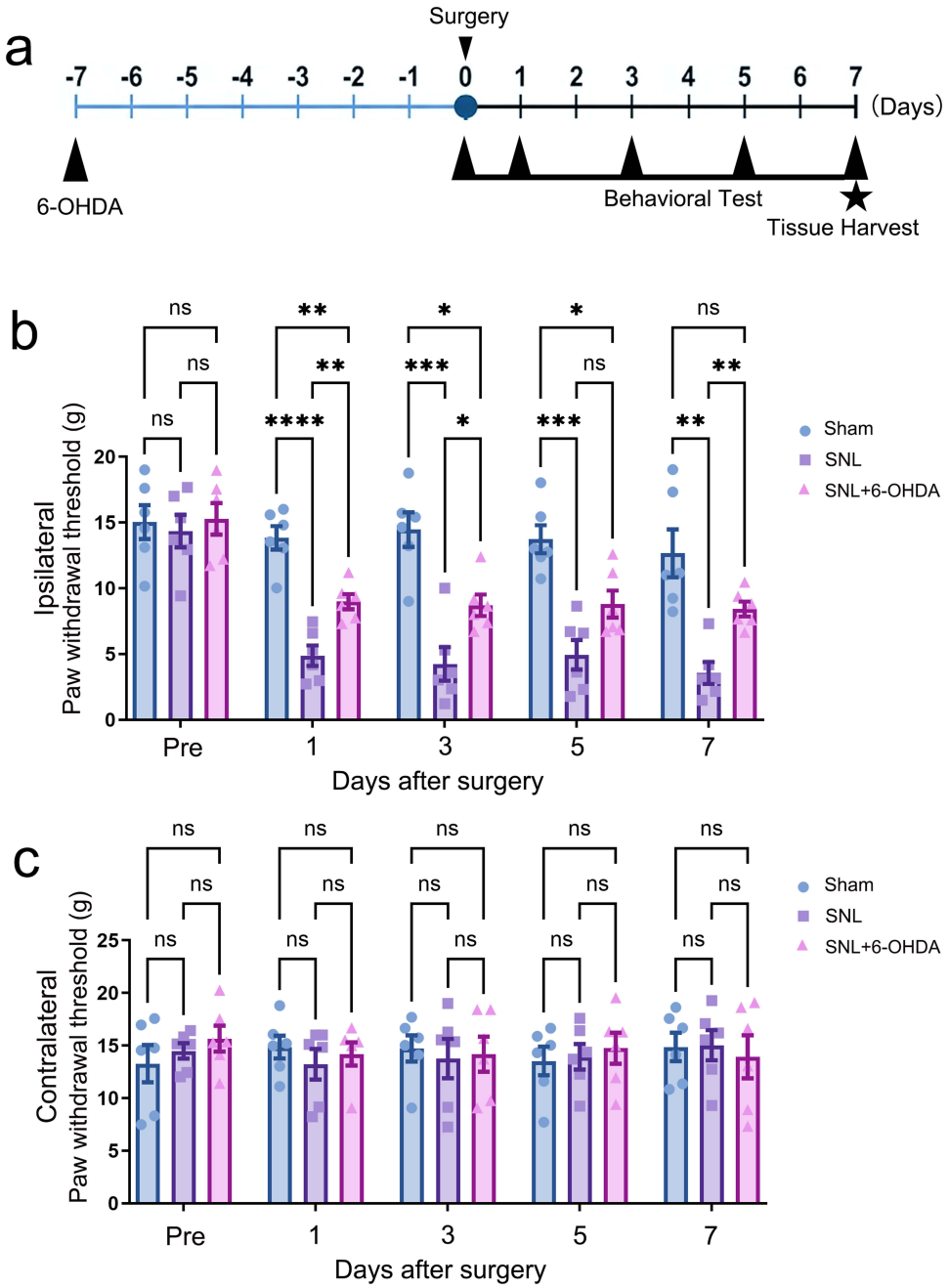

Figure 1 Systemic chemical sympathectomy attenuates SNL-induced mechanical allodynia. (**a**) Experimental timeline showing intraperitoneal 6-OHDA administration on day −7, SNL surgery on day 0, behavioral testing on postoperative days 1, 3, 5, and 7, and tissue harvest on day 7. (**b**) Ipsilateral paw withdrawal threshold (PWT) measured by von Frey testing. SNL reduced ipsilateral PWT, whereas preemptive 6-OHDA partially reversed SNL-induced mechanical allodynia. (**c**) Contralateral PWT measured over the same time course. Data are mean ± SD (n=6). Statistical brackets indicate the comparisons shown in the figure. ns, not significant; *p<0.05, **p<0.01, ***p<0.001, ****p<0.0001; two-way repeated-measures ANOVA followed by Tukey post hoc multiple comparisons.

phosphorylation in the spinal dorsal horn (Figure 3d). Quantification confirmed reductions in Iba-1 fluorescence (Figure 3e; Hedges' g=−3.19, 95% CI −4.94 to −1.45) and p-p38 fluorescence (Figure 3e; Hedges' g=−2.06, 95% CI −3.44 to −0.68). ELISA measurements further demonstrated decreased spinal TNF-α, IL-1β, and IL-6 levels after intrathecal P2Y12 blockade (Figure 3f).

https://doi.org/10.2147/JPR.S608956

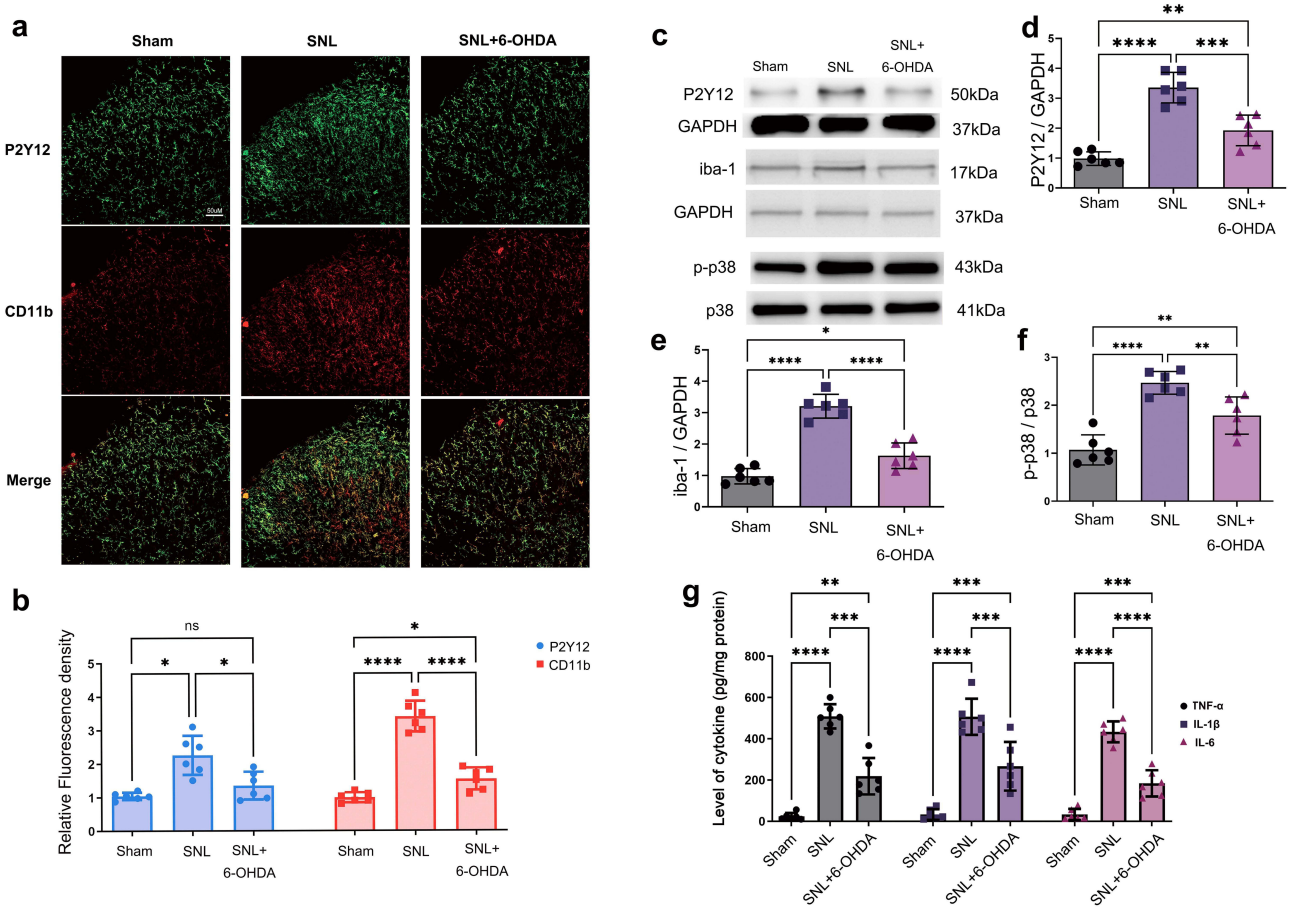

Figure 2 Peripheral sympathetic depletion reduces spinal microglial reactivity and P2Y12-p38 signaling. (**a**) Representative spinal dorsal horn immunofluorescence images showing P2Y12, CD11b, and merged labeling in Sham, SNL, and SNL + 6-OHDA groups. Scale bar=50 um. (**b**) Quantification of relative P2Y12 and CD11b fluorescence density. (**c**) Representative Western blot bands for P2Y12, Iba-1, p-p38, total p38, and loading controls. (**d**) Densitometric quantification of P2Y12/GAPDH. (**e**) Densitometric quantification of Iba-1/GAPDH. (**f**) Quantification of the p-p38/p38 ratio. (**g**) ELISA quantification of spinal TNF-α, IL-1β, and IL-6. Data are mean ± SD (n=4-6). Statistical brackets indicate the comparisons shown in the figure. *p<0.05, **p<0.01, ***p<0.001, ****p<0.0001; one-way ANOVA for single-marker and cytokine comparisons, followed by Tukey post hoc multiple comparisons.
Abbreviation: ns, not significant.

In vivo Pharmacological Occlusion Supports a Coupled Peripheral-to-Central Relationship

To test whether sympathetic drive and spinal P2Y12 signaling operate independently or within a shared functional pathway, we performed a pharmacological occlusion experiment. Ticagrelor alone did not alter baseline nociceptive thresholds in uninjured rats. After SNL, 6-OHDA, ticagrelor, and combined treatment each improved ipsilateral PWT compared with SNL. AUC analysis across the four nerve-injured groups showed larger cumulative thresholds in SNL + 6-OHDA (50.11±4.94 g.day; Hedges' g vs SNL=3.24, 95% CI 1.48 to 5.01), SNL + ticagrelor (55.83±10.79 g.day; Hedges' g vs SNL=2.88, 95% CI 1.24 to 4.52), and combined treatment (52.85±9.28 g.day; Hedges' g vs SNL=2.84, 95% CI 1.21 to 4.46) than in SNL alone (25.09±8.78 g.day). The combined intervention did not produce a statistically detectable additive or synergistic benefit compared with either monotherapy (Figure 4).

Schematic Model of the Trans-Compartmental Sympathetic-Microglial P2Y12 Axis

Based on the behavioral, biochemical, and pharmacological findings, we propose a working model of a peripheral-to-central sympathetic-microglial P2Y12 axis (Figure 5). In this model, SNL induces sympathetic sprouting within the DRG (Figure 5, step 1), which may increase noradrenaline exposure and promote sensory neuron ectopic firing (Figure 5, step 2). Hyperactive primary afferent input may then enhance ATP release within the spinal dorsal horn (Figure 5, step 3). Extracellular nucleotides engage microglial P2Y12 receptors and facilitate p38 MAPK signaling (Figure 5, step 4),

https://doi.org/10.2147/JPR.S608956

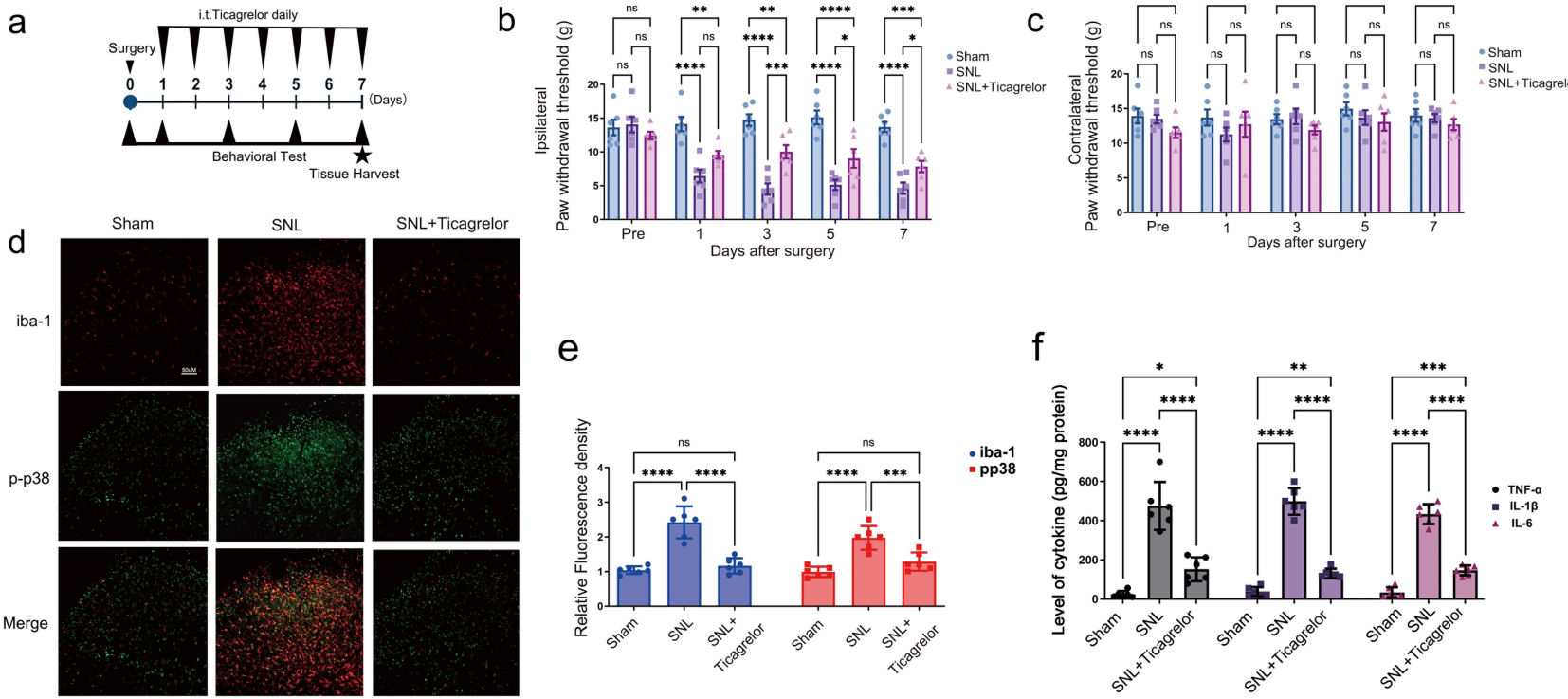

Figure 3 Intrathecal P2Y12 blockade attenuates neuropathic pain and spinal neuroinflammation. (**a**) Experimental timeline showing SNL surgery, daily intrathecal ticagrelor administration, behavioral testing, and tissue harvest. (**b**) Ipsilateral PWT after intrathecal ticagrelor. Ticagrelor attenuated SNL-induced mechanical allodynia. (**c**) Contralateral PWT after intrathecal ticagrelor. (**d**) Representative spinal dorsal horn immunofluorescence images showing Iba-1, p-p38, and merged labeling. Scale bar=50 um. (**e**) Quantification of relative Iba-1 and p-p38 fluorescence density. (**f**) ELISA quantification of spinal TNF-α, IL-1β, and IL-6. Data are mean ± SD (n=4-6). Statistical brackets indicate the comparisons shown in the figure. *p<0.05, **p<0.01, ***p<0.001, ****p<0.0001; two-way repeated-measures ANOVA for behavioral time-course data and one-way ANOVA for molecular/ELISA data, followed by Tukey post hoc multiple comparisons.

Abbreviation: ns, not significant.

https://doi.org/10.2147/JPR.S608956

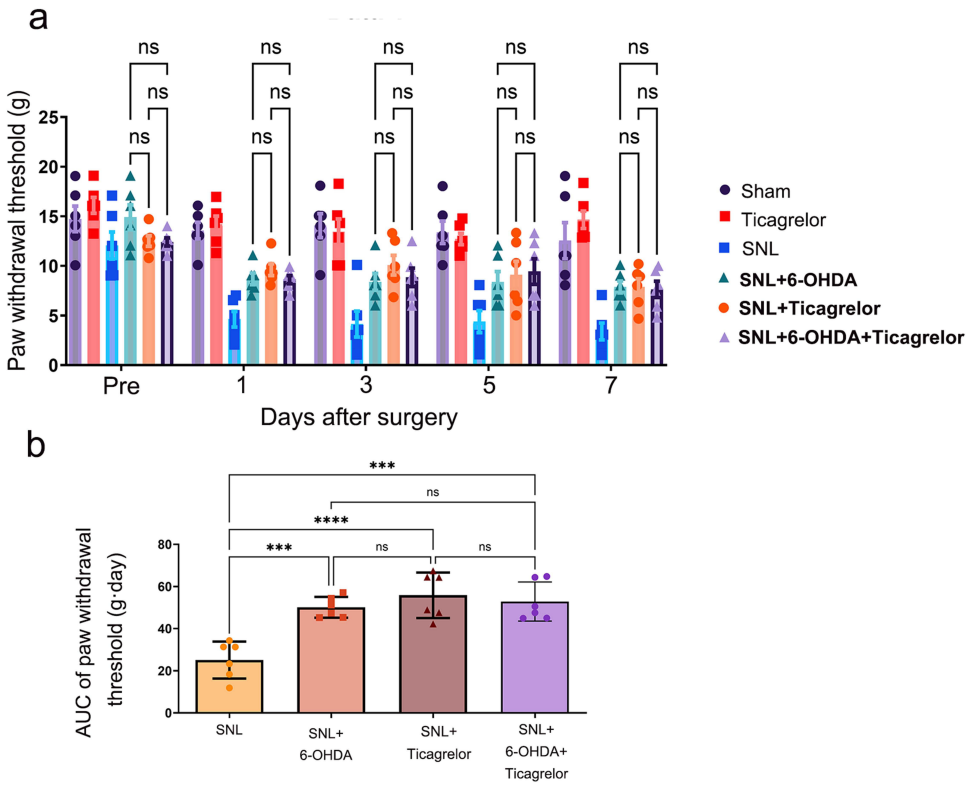

Figure 4 Pharmacological occlusion supports a coupled relationship between peripheral sympathetic drive and spinal P2Y12 signaling. (**a**) Time-course ipsilateral PWT across Sham, ticagrelor-only, SNL, SNL + 6-OHDA, SNL + ticagrelor, and SNL + combined 6-OHDA/ticagrelor groups. Ticagrelor-only did not alter baseline thresholds in uninjured rats. The intervention curves overlapped substantially, indicating no additional behavioral improvement with combined treatment. (**b**) AUC of ipsilateral PWT for the four nerve-injured groups. AUCs were 25.09±8.78, 50.11±4.94, 55.83±10.79, and 52.85±9.28 g.day for SNL, SNL + 6-OHDA, SNL + ticagrelor, and SNL + combined treatment, respectively. Data are mean ± SD (n=6). Statistical brackets indicate the comparisons shown in the figure. ***p<0.001, ****p<0.0001; two-way repeated-measures ANOVA for time-course data and one-way ANOVA for AUC comparisons, followed by Tukey post hoc multiple comparisons.
Abbreviation: ns, not significant.

followed by cytokine release that contributes to postsynaptic nociceptive sensitization (Figure 5, step 5). This model remains pharmacologically supported rather than definitively proven at every molecular relay, and additional cell-specific studies are needed to map the intermediate steps.

Discussion

This study provides pharmacological evidence that peripheral sympathetic activity amplifies spinal microglial P2Y12-p38 signaling in the rat SNL model. Peripheral 6-OHDA attenuated SNL-induced mechanical allodynia and suppressed spinal microglial reactivity, P2Y12/Iba-1 upregulation, p38 phosphorylation, and cytokine release. Intrathecal P2Y12 antagonism produced convergent behavioral and anti-inflammatory effects. The lack of an additive analgesic benefit with combined treatment supports a coupled peripheral-to-central relationship, although it should not be interpreted as definitive proof of every intermediate step in a serial molecular cascade.

A central conceptual challenge in SMP is reconciling peripheral sympathetic pathology with central glial activation.[15] In our design, 6-OHDA was administered 7 days before SNL, when the BSCB is expected to be relatively intact. This timing reduces the likelihood that post-injury barrier disruption allowed direct central 6-OHDA effects. Nevertheless, systemic 6-OHDA globally alters peripheral sympathetic tone, including sympathetic innervation of immune organs, as shown by splenic TH depletion.[16] Therefore, part of the observed spinal effect may reflect altered peripheral immune/autonomic signaling rather than only DRG-local sympathetic-sensory coupling.

P2Y12 should also be interpreted within the broader biology of microglia. Its canonical function is chemotaxis and early process extension toward extracellular nucleotides,[9] not obligatory direct induction of cytokine transcription.[11] The observed reductions in p-p38, TNF-α, IL-1β, and IL-6 after ticagrelor suggest that P2Y12 signaling is an important

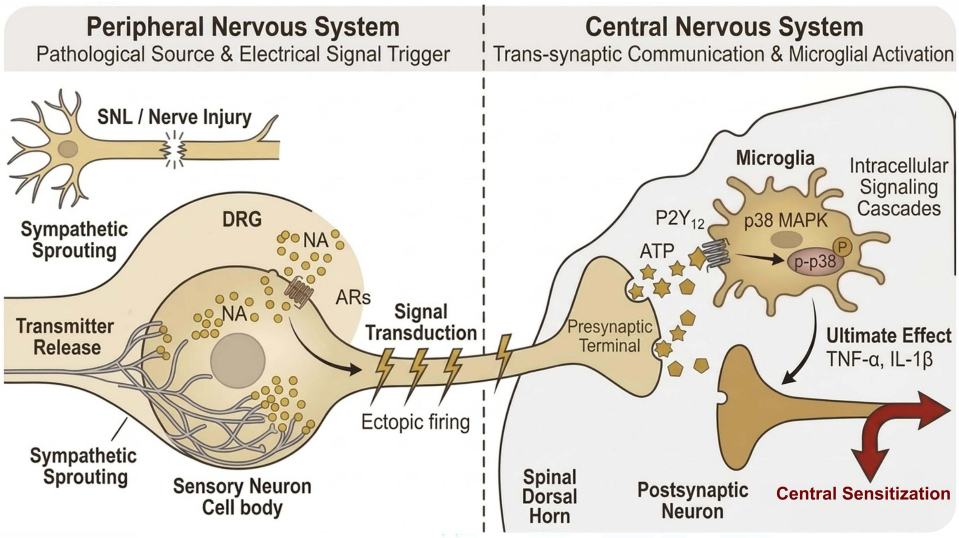

Figure 5 Schematic working model of the peripheral-to-central sympathetic-microglial P2Y12 axis. Step 1: SNL induces aberrant sympathetic sprouting within the DRG, leading to focal noradrenaline release. Step 2: Noradrenaline acts on adjacent primary sensory neurons and may promote ectopic firing. Step 3: Hyperactive primary afferent terminals release ATP in the spinal dorsal horn. Step 4: Extracellular ATP engages microglial P2Y12 receptors, promoting chemotaxis/morphological responses and facilitating p38 MAPK signaling. Step 5: Subsequent cytokine release contributes to postsynaptic nociceptive sensitization and maintenance of neuropathic pain. This model is pharmacologically supported but requires further validation of intermediate molecular relays.

upstream modulator in this model, but cytokine production is likely shaped by parallel purinergic, pattern-recognition, neuronal, astrocytic, and immune-cell pathways.[17,18] Accordingly, the present findings position P2Y12 as a therapeutically interesting interface rather than as a sole inflammatory switch.[19]

The occlusion experiment provides useful but bounded mechanistic inference. If peripheral sympathetic drive and spinal P2Y12 signaling were fully independent drivers, combined blockade would be expected to yield additive or synergistic analgesia. Instead, the combined treatment plateaued at a level similar to either monotherapy. This result is consistent with pharmacological epistasis, but alternative explanations remain possible, including ceiling effects inherent to von Frey behavior, maximal efficacy of either intervention, or off-target pharmacological actions. Genetic and cell-type-specific approaches will be required to resolve these alternatives.

Several limitations should be emphasized. First, the sympathectomy was preemptive and therefore models prevention of pathway development rather than reversal of established chronic pain. Second, the behavioral phenotype was assessed using mechanical allodynia only; thermal hyperalgesia, cold allodynia, and spontaneous pain were not examined. Third, CD11b and Iba-1 indicate microglial reactivity and morphology, but they do not define transcriptomic or functional microglial phenotypes. Fourth, ticagrelor was used as an experimental intrathecal P2Y12 antagonist and should not be interpreted as a directly translatable neuraxial therapy, given its antiplatelet effects, uncertain central pharmacokinetics, and potential off-target risks.

In conclusion, our findings support a functional peripheral-to-central neuroimmune model in which peripheral sympathetic activity acts as an upstream amplifier of spinal microglial P2Y12-p38 signaling in SNL-induced neuropathic pain. This framework may help explain why isolated peripheral or central interventions can be insufficient in SMP-like states.[20] Future work should validate the pathway in established pain, assess additional sensory modalities, and use cell-specific approaches to define the molecular relays linking DRG sympathetic-sensory coupling to spinal microglial signaling.

Conclusion

Peripheral sympathetic depletion and spinal P2Y12 antagonism each attenuated SNL-induced mechanical allodynia and neuroinflammatory signaling, while combined treatment produced no additional analgesic gain over monotherapy. These data support a pharmacologically coupled peripheral sympathetic-spinal microglial P2Y12 axis in this rat SNL model. The pathway should be interpreted as an important amplifier rather than a universal prerequisite for microglial activation, and its clinical relevance requires further validation.

https://doi.org/10.2147/JPR.S608956

Data Sharing Statement

The datasets generated and analyzed during the current study are available from the corresponding author on reasonable request.

Ethics Statement

All experiments involving animals were conducted in accordance with guidelines for laboratory animal care and use issued by the National Institutes of Health and the ARRIVE guidelines, and were approved by the Animal Care and Use Committee of the Sixth People's Hospital Affiliated to Shanghai Jiao Tong University (SYXK [Shanghai, China] 2021-0028).

Author Contributions

T.T.Y. conceptualized and designed the study, performed biochemical and Western blot analyses, analyzed data, and drafted the manuscript. Z.P.L. and H.H. conducted behavioral testing and assisted with data acquisition. H.Y. supervised the study, contributed to data interpretation, and revised and finalized the manuscript. All authors made a significant contribution to the work reported, whether in conception, study design, execution, acquisition of data, analysis and interpretation, or in all these areas; took part in drafting, revising, or critically reviewing the article; gave final approval of the version to be published; agreed on the journal to which the article has been submitted; and agree to be accountable for all aspects of the work.

Funding

This research was funded by the Scientific Research Fund of Shanghai Sixth People's Hospital (YNQN202219).

Disclosure

The authors declare no competing interests in this work.

References

1. Raja SN, Treede RD, Warner D. Testing the link between sympathetic efferent and sensory afferent fibers in neuropathic pain. *Anesthesiology*. 2012;117(1):173–177. doi:10.1097/ALN.0b013e31825adb2b
2. Chung K, Lee BH, Yoon YW, Chung JM. Sympathetic sprouting in the dorsal root ganglia of the injured peripheral nerve in a rat neuropathic pain model. *J Comp Neurol*. 1996;376(2):241–252. doi:10.1002/(SICI)1096-9861(19961209)376:2<241::AID-CNE6>3.0.CO;2-3
3. Xie W, Strong JA, Li H, Zhang JM. Sympathetic sprouting near sensory neurons after nerve injury occurs preferentially on spontaneously active cells and is reduced by early nerve block. *J Neurophysiol*. 2007;97(1):492–502. doi:10.1152/jn.00899.2006
4. McLachlan EM, Jänig W, Devor M, Michaelis M. Peripheral nerve injury triggers noradrenergic sprouting within dorsal root ganglia. *Nature*. 1993;363(6429):543–546. doi:10.1038/363543a0
5. Cui X, Zhang Z, Xi H, Liu K, Zhu B, Gao X. Sympathetic-sensory coupling as a potential mechanism for acupoints sensitization. *J Pain Res*. 2023;16:2997–3004. doi:10.2147/JPR.S424841
6. Ma YC, Kang ZB, Shi YQ, Ji WY, Zhou WM, Nan W. The complexity of neuropathic pain and central sensitization: exploring mechanisms and therapeutic prospects. *J Integr Neurosci*. 2024;23(5):89. doi:10.31083/j.jin2305089
7. Ji RR, Donnelly CR, Nedergaard M. Astrocytes in chronic pain and itch. *Nat Rev Neurosci*. 2019;20(11):667–685. doi:10.1038/s41583-019-0218-1
8. Prinz M, Masuda T, Wheeler MA, Quintana FJ. Microglia and central nervous system-associated macrophages-from origin to disease modulation. *Annu Rev Immunol*. 2021;39:251–277. doi:10.1146/annurev-immunol-093019-110159
9. Haynes SE, Hollopeter G, Yang G, et al. The P2Y12 receptor regulates microglial activation by extracellular nucleotides. *Nat Neurosci*. 2006;9(12):1512–1519. doi:10.1038/nn1805
10. Yu T, Zhang X, Shi H, et al. P2Y12 regulates microglia activation and excitatory synaptic transmission in spinal lamina II neurons during neuropathic pain in rodents. *Cell Death Dis*. 2019;10(3):165. doi:10.1038/s41419-019-1425-4
11. Inoue K, Tsuda M. Microglia in neuropathic pain: cellular and molecular mechanisms and therapeutic potential. *Nat Rev Neurosci*. 2018;19(3):138–152. doi:10.1038/nrn.2018.2
12. de Almodovar C R, Dupraz S, Bonanomi D. Neurovascular dynamics in the spinal cord from development to pathophysiology. *Neuron*. 2025;113(24):4134–4157.
13. Wulf MJ, Tom VJ. Consequences of spinal cord injury on the sympathetic nervous system. *Front Cell Neurosci*. 2023;17:999253. doi:10.3389/fncel.2023.999253
14. Chaplan SR, Bach FW, Pogrel JW, Chung JM, Yaksh TL. Quantitative assessment of tactile allodynia in the rat paw. *J Neurosci Methods*. 1994;53(1):55–63. doi:10.1016/0165-0270(94)90144-9
15. Ji RR, Nackley A, Huh Y, Terrando N, Maixner W. Neuroinflammation and central sensitization in chronic and widespread pain. *Anesthesiology*. 2018;129(2):343–366. doi:10.1097/ALN.0000000000002130
16. Mishra I, Pullum KB, Eads KN, Strunjas AR, Ashley NT. Peripheral sympathectomy alters neuroinflammatory and microglial responses to sleep fragmentation in female mice. *Neuroscience*. 2022;505:111–124. doi:10.1016/j.neuroscience.2022.09.022

17. Salter MW, Beggs S. Sublime microglia: expanding roles for The Guardians of the CNS. *Cell*. 2014;158(1):15–24. doi:10.1016/j.cell.2014.06.008
18. Boadas-Vaello P, Castany S, Homs J, Álvarez-Pérez B, Deulofeu M, Verdú E. Neuroplasticity of ascending and descending pathways after somatosensory system injury: reviewing knowledge to identify neuropathic pain therapeutic targets. *Spinal Cord*. 2016;54(5):330–340. doi:10.1038/sc.2015.225
19. Tozaki-Saitoh H, Tsuda M, Miyata H, Ueda K, Kohsaka S, Inoue K. P2Y12 receptors in spinal microglia are required for neuropathic pain after peripheral nerve injury. *J Neurosci*. 2008;28(19):4949–4956. doi:10.1523/JNEUROSCI.0323-08.2008
20. Zhang JH, Deng YP, Geng MJ. Efficacy of the lumbar sympathetic ganglion block in lower limb pain and its application prospects during the perioperative period. *Ibrain*. 2022;8(4):442–452. doi:10.1002/ibra.12069